Theor Chem Acc (2011) 129:367–379
DOI 10.1007/s00214-010-0855-y

REGULAR ARTICLE

Improved valence basis sets for divalent lanthanide 4f-in-core pseudopotentials

Michael Hülsen · Michael Dolg · Pascal Link · Uwe Ruschewitz

Received: 15 October 2010 / Accepted: 4 November 2010 / Published online: 26 November 2010

Abstract Improved energy-optimized (6s5p4d) and (7s6p5d) primitive valence basis sets have been derived for energy-consistent scalar-relativistic 4f-in-core pseudopotentials of the Stuttgart-Cologne variety modeling divalent lanthanides with a $4f^{n+1}$ occupation (n = 0–13 for La–Yb). Segmented contracted basis sets covering the range of polarized double-, triple-, and quadruple-zeta quality, augmented by 2f1g correlation sets, were created for use in molecular calculations. The basis sets contain smaller (4s4p3d) and (5s5p4d) primitive subsets, which are designed in particular for solid state calculations of crystals containing divalent lanthanide ions. Hartree–Fock, density functional theory and coupled cluster results obtained with the new basis sets for lanthanide atomic ionization potentials as well as of geometry optimizations of various test molecules, i.e. selected lanthanide mono- and dihydrides, mono- and difluorides, and monooxides, show a satisfactory agreement with experimental data as well as with corresponding scalar-relativistic all-electron results. Core-polarization potentials are found to improve the results, especially for the atomic first and second ionization potentials.

Keywords Lanthanides · Valence basis sets · Pseudopotentials · Divalent lanthanide compounds · Core-polarization potentials

1 Introduction

Electronic structure calculations of lanthanide compounds often encounter difficulties due to the large contributions of relativity [1] as well as of electron correlation [2, 3]. In addition, the presence of open 4f shells frequently leads to additional problems, e.g. a large number of low-lying electronic states, many of which require a multi-reference wavefunction, possibly also adapted to spin-orbit effects, for a proper description. The pseudopotential (PP) approach, possibly combined with the effective core-polarization potential (CPP) approach, is a widely used method in relativistic quantum chemistry to reduce the computational effort of a calculation by restricting the explicit quantum treatment to the valence shell. In addition, it also allows to include the major relativistic effects into the formally non-relativistic calculations implicitly by a proper adjustment of free parameters in the valence-only model Hamiltonian. Besides the widely used shape-consistent PPs, e.g. the main group and transition metal sets provided by Hay and Wadt [4–6], the energy-consistent PP variety is quite frequently used [7, 8]. For the lanthanides, two types of energy-consistent PPs with different core definitions are available. On the one hand, 4f-in-valence [9, 10] PPs and on the other hand 4f-in-core [12–14] PPs.

Dedicated to Professor Pekka Pyykkö on the occasion of his 70th birthday and published as part of the Pyykkö Festschrift Issue.

Electronic supplementary material The online version of this article (doi:10.1007/s00214-010-0855-y) contains supplementary material, which is available to authorized users.

M. Hülsen · M. Dolg (✉)
Institute for Theoretical Chemistry, University of Cologne, Greinstr. 4, 50939 Cologne, Germany
e-mail: m.dolg@uni-koeln.de

M. Hülsen
e-mail: huelsenm@uni-koeln.de

P. Link · U. Ruschewitz
Institute for Inorganic Chemistry, University of Cologne, Greinstr. 6, 50939 Cologne, Germany
e-mail: uwe.ruschewitz@uni-koeln.de

The first set uses a small PP core ($1s^2-3d^{10}$) in order to avoid significant frozen-core errors, which mainly arise when the occupation of the very compact 4f shell, which is buried quite deeply in the core, is changed. In contrast to these potentially quite accurate small-core PPs (SPPs), the PPs of the second set, sometimes also called large-core PPs (LPPs), avoid many problems which arise from a partially occupied 4f shell by attributing it to the PP core. In this case, the core has to be chosen in such a way that the sometimes partially occupied 5d shell is outside the core ($1s^2-4f^n$) and frozen-core errors due to changes of its occupation are acceptable small. A related 5f-in-core PP ansatz was recently devised and quite successfully tested for the actinides [15–17]. The f-in-core PPs were the first PPs published for lanthanides at a time, when relativistic first-principles calculations on f-element systems, especially the lanthanides, were still scarce [18]. They still remain computationally attractive due to the large difficulties arising for a rigorous explicit treatment of partially occupied f shells.

The f-in-core PP approach for lanthanide and actinide compounds is frequently successful due to the core-like behaviour of the f shells and their usually only weak direct participation in chemical bonding. Since a f shell with a fixed number of electrons is included in the PP core, each f-in-core PP corresponds to a specific oxidation state of an atom. The aim to make the approach efficient by the usage of relatively small valence basis sets leads to the optimization of individual basis sets for every oxidation state of each lanthanide or actinide element. Improved valence basis sets for molecular calculations together with compact basis sets for crystal orbital calculations were created for the tri- [12, 13] and tetravalent [14] LPPs of the lanthanides during the last years [14, 19, 20]. The derivation of 5f-in-core actinide PPs together with corresponding molecular and crystal basis sets was completed recently for di-[16], tri-[15], tetra-[16], penta-[17], and hexavalent [17] LPPs for Pu–No, Ac–Lr, Th–Cf, Pa–Am, and U–Am, respectively.

In this contribution, we present optimized molecular and crystal valence basis sets for the divalent lanthanide LPPs [12, 13] and hereby complete the set of f-in-core PPs and basis sets for lanthanides and actinides. In order to inspect the quality of the new valence basis sets, a wide variety of test calculations was performed. Results for ionization potentials (IPs) of the lanthanide atoms from La to Yb as well as for miscellaneous molecular test systems (LnX_n, Ln=Sm, Eu, Tm, Yb; X=H, F; $n = 1, 2$; EuO, YbO) are compared to experimental data, to results of previous work as well as to those of scalar-relativistic all-electron calculations. In addition, crystal orbital calculations on the dicarbides of Yb and Eu, i.e. EuC_2 and YbC_2, are reported and the lanthanide oxidation state in these systems is discussed.

2 Methods

The method of relativistic energy-consistent ab initio PPs is described in detail elsewhere [8, 9, 12] and will be outlined here only briefly. The valence-only model Hamiltonian for a quantum mechanical system of n electrons and N cores with an effective core charge Q is given by

$$H_v = -\frac{1}{2}\sum_i^n \Delta_i + \sum_{i<j}^n \frac{1}{r_{ij}} + \sum_i^n \sum_I^N V_I(r_i) + \sum_{i<j}^N \frac{Q_I Q_J}{R_{IJ}} + V_{\mathrm{CPP}} \,. \quad (1)$$

Electron indices are denoted by i and j, and core indices by I and J, respectively. The semi-local PP $V_I(r_i)$ of a core I is given by

$$V_I(r_i) = -\sum_i^n \frac{Q_I}{r_{Ii}} + \sum_i^n \sum_{lk} A_{lk}^I \exp(-a_{lk}^I r_i^2) P_l^I \,. \quad (2)$$

A_{lk} and a_{lk} are free parameters, which are adjusted during the creation of the pseudopotential (PP) by reproducing the total valence energies of several low-lying states of the corresponding neutral atom and its ions [12]. $P^I{}_l$ denotes the projection operator onto the Hilbert subspace of core I with angular momentum l

$$P_l^I = \sum_{m_l} |lm_l\rangle\langle lm_l| \,. \quad (3)$$

Since 4f-in-core PPs model near-integral 4f occupations for the lanthanides, one needs a distinct PP for every valency of an atom (divalent: $4f^{n+1}$, n = 0–13 for La–Yb; trivalent: $4f^n$, n = 0–14 for La–Lu; tetravalent: $4f^{n-1}$, $n = 1, 2, 3, 8, 9$ for Ce, Pr, Nd, Tb, Dy). The shells from 1s to 4f are included in the PP core. Orbitals with a main quantum number larger than 4 are treated explicitly as valence shells. The whole PP consists of s, p, and d radial potentials, each composed of two Gaussian functions and a f radial potential represented by one Gaussian. The exponents and coefficients of the Gaussian functions were energy-adjusted to all-electron (AE) calculations using the Wood–Boring (WB) scalar-relativistic Hartree–Fock (HF) approach [11–14].

The optimization of segmented contracted cartesian Gaussian function valence basis sets for the 4f-in-core PPs of divalent lanthanides aimed to obtain sets without diffuse functions suitable for crystal orbital calculations as well as sets with diffuse functions suitable for molecular orbital calculations and containing the former as subsets.

First two different primitive Gaussian sets, (4s4p3d) and (5s5p4d), were energy-optimized using the atomic HF program ATMSCF [21] and form the starting point for compact contracted crystal orbital basis sets. At first, uncontracted (4s4p) and (5s5p) basis functions were energy-optimized for the $Ln^{2+}5s^25p^6$ valence subconfiguration of the $4f^{n+1}$ core subconfiguration corresponding to divalent lanthanides. The exponents of the (3d) and (4d) basis were then energy-optimized for the $Ln^{+}5s^25p^65d^1$ valence subconfiguration keeping the s and p exponents unchanged. In order to prevent numerical problems arising from linear dependencies in condensed phase calculations, the diffusest d-exponent was fixed to a value of 0.15. The ratio between two basis functions of the same angular symmetry was required to be at least 1.5, in order to avoid nearly coinciding exponents with very large contraction coefficients of opposite sign.

The derived (4s4p3d) and (5s5p4d) valence basis sets were then extended by adding a set of diffuse (2s1p1d) functions to produce (6s5p4d) and (7s6p5d) primitive sets as suitable starting points for molecular basis sets. The exponents of these new functions were energy-optimized for the $5s^25p^66s^2$ (s-basis), $5s^25p^66s^16p^1$ (p-basis) and $5s^25p^65d^16s^1$ (d-basis) valence subconfigurations of neutral lanthanide atoms. The valence basis sets were then contracted using different segmented contraction patterns in order to receive basis sets covering approximately the range of valence double-, triple-, and quadruple-zeta quality. The resulting contracted valence basis sets are (4s4p3d)/[2s2p2d], (4s4p3d)/[3s3p2d], (5s5p4d)/[2s2p2d], (5s5p4d)/[3s3p3d], and (5s5p4d)/[4s4p3d] for crystal orbital calculations as well as (6s5p4d)/[4s3p3d], (6s5p4d)/[5s4p3d], (7s6p5d)/[4s3p3d], (7s6p5d)/[5s4p4d], and (7s6p5d)/[6s5p4d] for molecular orbital calculations.

Finally, sets of 2f1g polarization functions were energy-optimized in configuration interaction (CI) calculations [22] for a $5s^25p^66s^2$ lanthanide valence subconfiguration. Note that this case corresponds to the atomic ground state configuration of all neutral lanthanide atoms except for La, Ce, Gd and Lu, where the atomic ground state 4f subconfiguration corresponds to the trivalent situation. A complete list of basis set parameters is provided in the electronic supplementary material and is also available through the authors' PP basis set library [23].

Core-polarization potentials (CPPs) [24]

$$V_{\mathrm{CPP}} = \frac{1}{2}\sum_{\lambda}^{N} \alpha_D^{\lambda} \mathbf{f}_{\lambda}^{\,2} \tag{4}$$

using a Meyer-type cutoff-factor $\omega(r)$ [25, 26] for the electrostatic field

$$\mathbf{f}_{\lambda} = \sum_{i}^{n} \frac{\mathbf{r}_{i\lambda}}{r_{i\lambda}^3}\omega(r_{i\lambda}) - \sum_{\substack{\mu \\ \mu\neq\lambda}}^{N} Q_{\mu\lambda}\frac{\mathbf{r}_{\mu\lambda}}{r_{\mu\lambda}^3}\omega(r_{\mu\lambda})$$
$$\text{with } \omega(r) = (1-\exp(-\delta r^2)). \tag{5}$$

were used in the PP calculations of this work. CPPs implicitly cover both static and dynamic polarization of the PP core and were found to be an important extension for the 4f-in-core PPs. The dipole polarizabilities α_D of the PP cores used in the CPPs were determined by interpolation of the Dirac–Hartree–Fock (DHF) dipole polarizabilites α_D of the closed-shell cores Ba^{10+} (0.5631 au) and Yb^{10+} (4.2745 au). The cutoff-parameter δ was fitted to the experimental values of the first and second ionization potentials of Yb ($\delta = 0.4589$) and used for all other atoms.

All atomic and molecular test calculations were carried out with the MOLPRO program package version 2006.1 [22], whereas for the crystalline solid calculations the program CRYSTAL06 [27] was used. Besides calculations of the first and second atomic ionization potentials of selected lanthanides (Pr–Eu and Tb–Yb), where the initial and final states can be described by the divalent 4f-in-core PPs, also molecular test calculations were performed on all LnH, LnH_2, LnF, LnF_2, and LnO systems, where Ln is assumed to be in a divalent state (cf. supplementary material). For the discussion below we only consider those cases were a divalent Ln might be present in the ground state or at least a low-lying excited state, i.e. LnH, LnH_2, LnF, LnF_2 (Ln=Sm, Eu, Tm, Yb), and LnO (Ln=Eu, Yb). The calculations of the ionization potentials of the lanthanide atoms were performed with the uncontracted (7s6p5d) + 2f1g valence basis sets with and without inclusion of CPPs [24] at the coupled cluster singles and doubles level with a perturbative treatment of triples (CCSD(T)). The results are compared to experimental data [28] as well as values from previous small-core pseudopotential (SPP) complete active space self-consistent field (CASSCF) and subsequent averaged coupled pair-functional (ACPF) calculations [10]. The LPP HF, CCSD(T), and PBE0 (Perdew-Burke-Ernzerhof) gradient-corrected hybrid DFT [29, 30] geometry optimizations of the molecular model systems listed above applied (7s6p5d)/[6s5p4d] + 2f1g valence basis sets of VQZ quality for the lanthanides. For hydrogen, fluorine, and oxygen, Dunning's augmented correlation-consistent polarized VQZ (aug-cc-pVQZ) basis sets were used [31, 32]. The LnX_n bond energies E_{Ln-X} were calculated with respect to the separated atoms according to

$$E_{Ln-X} = \frac{1}{n}(E(Ln) + n\cdot E(X) - E(LnX_n))\,, \tag{6}$$

where $E(Ln)$, $E(X)$, and $E(LnX_n)$ denote the total (valence) energies.

Since experimental values for comparison are very scarce, we also performed PBE0 DFT [29, 30] calculations together with the Douglas–Kroll–Hess (DKH) second-order scalar-relativistic all-electron (AE) Hamiltonian [33, 34] for LnH, LnH_2, LnF, LnF_2 (Ln=Sm, Eu, Tm, Yb) and LnO (Ln=Eu, Yb). Due to the closed 4f shell, we were able to perform AE DKH CCSD(T) calculations for the Yb systems. The Yb 4f, 5s, 5p, 6s, O and F 2s, 2p and H 1s shells were kept active at the AE level. Segmented contracted (23s16p12d6f3g)/[18s12p9d3f3g] basis sets were applied in the AE calculations for the lanthanides [35], whereas aug-cc-pVQZ [31, 32] and aug-cc-pVQZ-DK [36] basis sets were used for H, O, and F in the PP and AE DKH calculations, respectively. Since the AE DKH Ln basis sets are relatively small, the binding and bond energies were corrected for the basis set superposition error with the Boys-Bernardi counter-poise prescription [37].

The (5s5p4d) valence basis sets for calculations of crystalline systems were recently applied to investigate structures and properties of solid lanthanide dicarbide systems LnC_2 [38]. Special emphasis was given to the question of the valency of europium and ytterbium in these compounds (+II vs. +III). A brief summary of these calculations is given here in order to illustrate the usage of the di- and trivalent lanthanide PPs as well as the corresponding newly optimized crystal orbital valence basis sets. For a discussion of the performance of the solid state basis sets for the trivalent lanthanide PPs the reader is referred to a previously published article [19], whereas the calculations on EuC_2 and YbC_2 will be discussed in more detail together with the experimental work on the YbC_2 system in a forthcoming publication [38].

3 Results and discussion

In the following, the quality of the new valence basis sets is assessed by comparing results of atomic and molecular test calculations to reference data from more rigorous calculations as well as to experimental data.

3.1 Valence basis sets

The total valence energies obtained with the primitive (4s4p3d) and (5s5p4d) valence basis sets was compared to reference values from finite-difference PP HF calculations for La to YbC, i.e. to the HF limit. The deviations for $Ln^+5s^25p^65d^1$ are shown in Fig. 1. It is seen that the smaller (4s4p3d) sets lead to errors increasing quickly along the lanthanide series with a maximum value of 1.54 eV at Yb. The larger (5s5p4d) sets provide a more uniform quality along the lanthanide series and lead to a significantly smaller maximum error of 0.48 eV at Yb. The

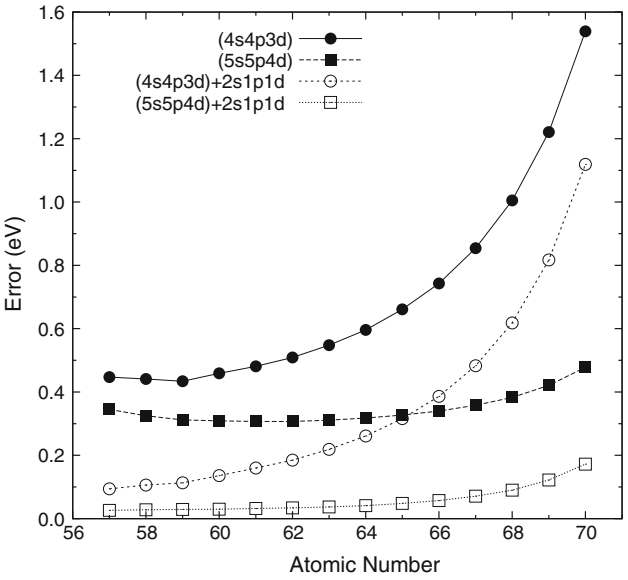

Fig. 1 Errors in the total valence energy (eV) with respect to the Hartree-Fock limit[a] for calculations of the singly charged lanthanide ions Ln^+ with a $5s^25p^65d^1$ valence subconfiguration using the primitive basis sets[b] and of the neutral lanthanide atoms Ln with a $5s^25p^65d^16s^1$ valence subconfiguration using the augmented primitive basis sets[c]. [a]Finite-difference HF calculations using the program MCHF [11]. [b]Algebraic HF calculations using the program ATMSCF [21]. [c]Algebraic HF calculations using the program MOLPRO [22]

mean absolute errors (m.a.e.) for La to Yb are 0.71 and 0.35 eV for the smaller and larger sets, respectively. We note that the applied primitive basis sets were designed for applications in calculations of crystalline solids containing Ln^{2+} ions and that in order to avoid linear dependencies in such calculations the exponential parameters were restricted to be larger than 0.15.

The quality of the augmented primitive (6s5p4d) and (7s6p5d) basis sets was checked for the neutral lanthanide atoms with a $5s^25p^65d^16s^1$ valence subconfiguration. Although most lanthanides (Pr–Eu,Tb–Yb) have a $5s^25p^66s^2$ ground state configuration, we use this excited configuration in order to probe the quality of the d basis set. The errors with respect to the HF limit are displayed in Fig. 1. Whereas the smaller (6s5p4d) sets still show a quick increase in the errors along the lanthanide series with a maximum of 1.12 eV at Yb, the larger (7s6p5d) sets show only a slow increase in the errors toward the end of the series with a maximum value of 0.17 eV at Yb. The m.a.e. are 0.36 and 0.06 eV for the smaller and larger sets, respectively. For the $5s^25p^66s^2$ valence subconfiguration the errors with respect to the HF limit are reduced by a factor of 10 when the new (7s6p5d) primitive set replaces the original set [12], i.e. the maximum deviations at Yb are 0.14 and 1.68 eV for the new and old set, respectively. The magnitude of the errors introduced by the new larger sets

corresponds roughly to the errors related to the PPs, when comparing to the AE WB reference values. Thus a further improvement of the basis sets would not lead to a reduction in the overall errors.

The errors due to the basis set contraction are displayed in Fig. 2 for the augmented (6s5p4d) and (7s6p5d) basis sets. The differences between the total energies of HF calculations with contracted and uncontracted basis sets stay below 0.01 and 0.007 eV for [4s3p3d] and [5s4p4d] when contracting the smaller (6s5p4d) primitive sets. The contraction errors for the larger (7s6p5d) valence basis sets are of comparable magnitude and below 0.03, 0.01 and 0.001 eV for the [4s3p3d], [5s4p4d] and [6s5p4d] contractions, respectively. In summary, at the HF level the errors are largely determined by the underlying primitive set and not so much by the contraction pattern itself.

3.2 Ionization potentials

The first (IP_1) and second (IP_2) ionization potentials are suitable for atomic test calculations using the divalent 4f-in-core PPs for the lanthanides together with the new valence basis sets. For the lanthanides from Pr to Eu and Tb to Yb, the first and second ionization of the neutral atoms consists of the removal of the outermost s electrons ($6s^2 \rightarrow 6s^1$ and $6s^1 \rightarrow 6s^0$), i.e., the 4f occupation remains the same after ionization of the atom and corresponds to the core occupation of the divalent 4f-in-core large-core PPs

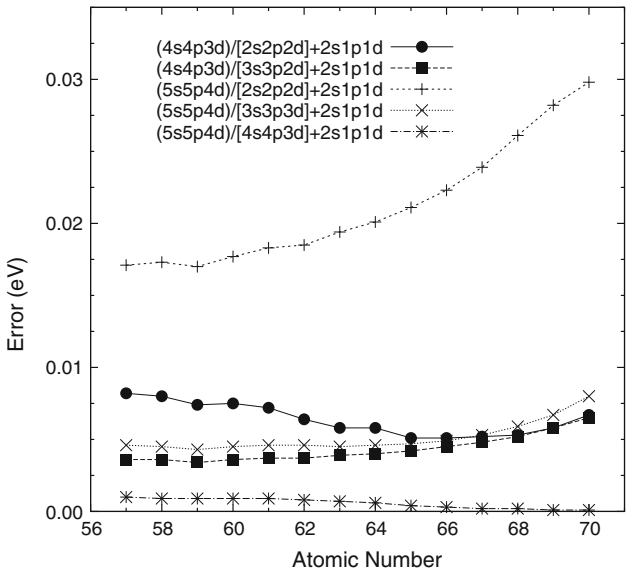

Fig. 2 Total energy differences between calculations with the contracted augmented (4s4p3d) + 2s1p1d and (5s5p4d) + 2s1p1d basis sets[a] and the corresponding uncontracted augmented basis sets[a] for neutral lanthanide atoms Ln with a $5s^25p^65d^16s^1$ valence subconfiguration. [a]SCF calculations using the program MOLPRO [22]

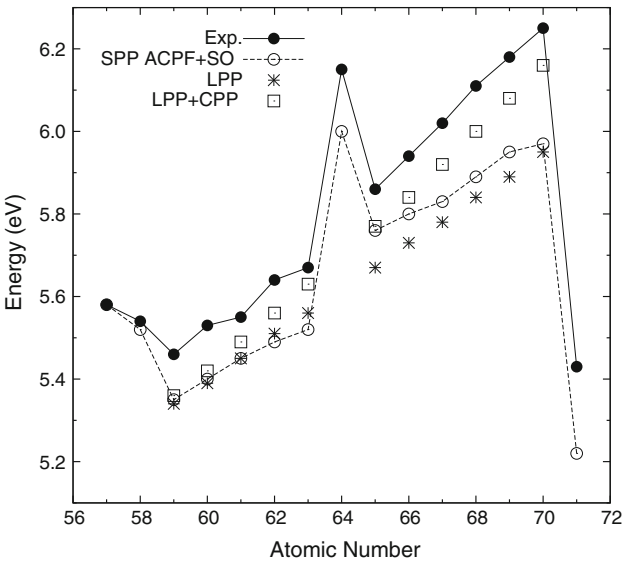

Fig. 3 Experimental first ionization potentials of the lanthanides Pr–Eu and Tb–Yb in comparison with the results of LPP CCSD(T) calculations[a] excluding and including a CPP and SPP ACPF + SO calculations [10] and experimental data [28]

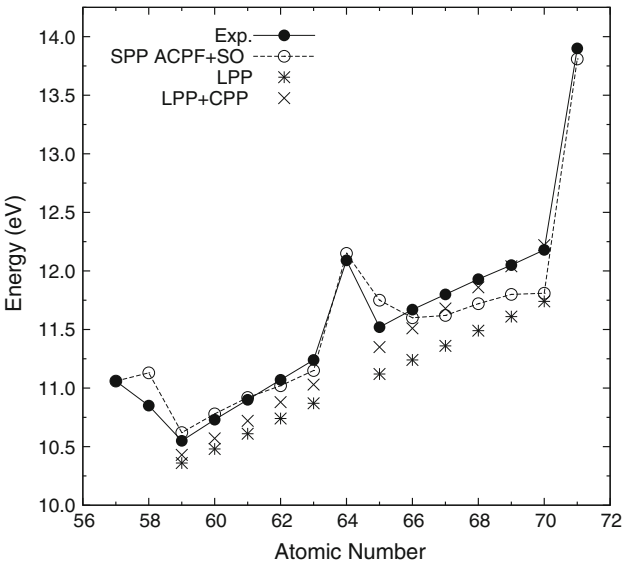

Fig. 4 As Fig. 3, but for the second ionization potentials of Pr–Eu and Tb–Yb

(LPPs). The calculated IPs are plotted in Figs. 3 and 4 together with the experimental values [10] and spin-orbit corrected 4f-in-valence small-core PP (SPP) ACPF results [28].

It can be seen that the SPP ACPF calculations reproduce the trend of the values of the ionization energies very well. The mean absolute errors are only 0.15 and 0.14 eV for IP_1 and IP_2, respectively, with maximum deviations of 0.28 and 0.37 eV, both for Yb. A large part of the deviations is probably due to an insufficient treatment of electron

correlation, i.e. for IP_3 and IP_4 it could be demonstrated that basis set extrapolated and spin-orbit corrected CCSD(T) results agree within 0.1 eV with the experimental values. In comparison, calculations using LPPs without CPPs result in errors of 0.19 eV (IP_1) and 0.37 eV (IP_2) with maximum differences of 0.30 eV for Yb and 0.44 eV for Ho, Er, Tm, and Yb, respectively. The usage of CPPs improves the results and deviations from experimental results become smaller. Analogously, one gets a mean absolute error of 0.09 eV (IP_1) and 0.13 eV (IP_2) with a maximum deviation of 0.11 eV for Nd and Er and 0.21 eV for Eu, respectively. This is close to the desired accuracy and documents the quality of the LPPs.

3.3 Molecular test calculations

Molecular test calculations have been performed for LnH_n, LnF_n and LnO (Ln=La–Yb, $n = 1, 2$) at the CCSD(T) level without and for selected systems with inclusion of a CPP. A complete list of the results of HF and CCSD(T) PP and PP + CPP calculations including bond lengths, bond angles, and dissociation energies can be found in the supplementary material. The following discussion however is restricted to those elements were a divalent metal ion is most likely, i.e. Sm and Eu as well as Tm and Yb, and includes PP + CPP PBE0 DFT results obtained for these cases. We adopt the concept of superconfigurations [39] in the following discussion, which is in line with the 4f-in-core PP approach. The AE DKH PBE0 results presented here however correspond to the lowest energy high-spin Kohn-Sham determinant.

Some of the molecules discussed here have been studied previously, partly by other authors and methods. Aside from LPP studies of LnX (Ln=La–Lu, X=H, O, F) and LnF_2 (Ln=Eu, Yb) using the originally published valence basis sets [13, 40, 41], the Stuttgart-Cologne SPPs have been used to calculate ground and low-lying electronic states of EuO [42, 43], YbO [43, 44], YbH and YbF [43, 45] at the multi-reference configuration interaction (MRCI) level, partly also including spin-orbit corrections [46]. Schwarz and coworkers applied the Amsterdam quasirelativistic AE approach (AMOL) to investigate YbO, YbH, and YbF at the density functional level [47, 48]. EuO, YbO, YbH and YbF were investigated at the 4-component Dirac-Kohn-Sham density functional theory (DFT) level using the Beijing density functional code (BDF) [49, 50]. Heiberg et al. [51] studied EuF, YbF, and YbH at the AE DKH CCSD(T) level using [9s8p6d4f3g] contracted basis sets for the lanthanides and cc-pVTZ basis sets for H and F. They also published B3LYP, BLYP, and BP86 results for the Stuttgart-Cologne LPPs and SPPs as well as the Amsterdam-Toulouse zeroth-order regular approximation (ZORA) as implemented in the Amsterdam density functional code (ADF). Wu et al. [52] performed B3LYP calculations for the whole LnO, LnO^+ and LnO^- series using the Stuttgart-Cologne SPPs. Their results for EuO and YbO can be compared to the present results. Andrews and coworkers investigated experimentally as well as theoretically lanthanide hydrides [53] using the Stuttgart-Cologne SPPs at the BP86, PBE and PBE0 DFT level.

In view of the uncertainties introduced when comparing results from different DFT parametrizations, we only use the AE DKH CCSD(T) results of Heiberg et al. [51] in addition to the corresponding results of this work for calibrating the PP + CPP CCSD(T) results. Similarly, we only use the AE DKH PBE0 results obtained in this work to calibrate the PP + CPP PBE0 results. When comparing to experimental values, one might hope that spin-orbit effects are negligible for the bond distances and angles, and largely cancel when calculating binding energies, since the lanthanide atom has the same 4f occupation in the atomic and molecular (ground) states. Note that the non-4f unpaired electrons are situated in σ orbitals for LnH and LnF, whereas all other molecules have a closed-shell configuration aside from the 4f shell. The same is true for the ground states of Sm, Eu, Tm, and Yb, whereas spin-orbit contributions of O and F are negligible for the present study.

3.3.1 Lanthanide monooxides

The results for the monoxides EuO and YbO are listed in Table 1. According to an ionic picture, i.e. $Eu^{2+}O^{2-}$ and $Yb^{2+}O^{2-}$, it should be possible to describe both systems by f-in-core PPs for divalent Eu and Yb as 18 valence electron systems. Whereas the $^8\Sigma^-$ ground state of EuO arises from a $[4f^7]\sigma^2\sigma^2\pi^4$ superconfiguration [42], the $^1\Sigma^+$ ground state of YbO might actually be due to a mixture of the $[4f^{14}]\sigma^2\sigma^2\pi^4$ and $[4f^{13}]\sigma^2\sigma^2\sigma^1\pi^4$ superconfigurations [44, 54]. Indeed, the present AE DKH CCSD(T) calculations actually yield a $^3\Sigma^+$ state ($R_e = 1.793$ Å, $D_e = 3.66/3.51$ eV without/with counter-poise correction) arising from the $[4f^{13}]\sigma^2\sigma^2\sigma^1\pi^4$ superconfiguration 0.39 eV below the $^1\Sigma^+$ state with the $[4f^{14}]\sigma^2\sigma^2\pi^4$ superconfiguration. This result agrees quite well with the original SPP MRCI result of 0.52 eV [45, 54]. With 4f-in-core PPs one cannot account for such complex electronic situations and thus we consider only the $[4f^{n+1}]\sigma^2\sigma^2\pi^4$ superconfigurations and a closed shell $^1\Sigma^+$ valence substate.

The PP + CPP PBE0 bond lengths are 0.03–0.04 Å larger than the DKH PBE0 values, whereas the PP + CPP PBE0 binding energies are 0.5–0.6 eV (10–15%) smaller than the DKH PBE0 results. Both the DKH PBE0 and the PP + CPP PBE0 bond length of YbO are longer than the

Table 1 Bond lengths R_e (in Å) and binding energies D_e (in eV) of selected lanthanide monoxides LnO from PP(+CPP) CCSD(T) and PBE0 calculations in comparison with all-electron (AE) DKH2 PBE0 results without/with counter-poise correction of the basis set superposition error

Ln	R_e				D_e			
	CCSD(T)		PBE0		CCSD(T)		PBE0	
	PP	PP + CPP	PP + CPP	DKH	PP	PP + CPP	PP + CPP	DKH
Eu	1.920	1.918	1.889	1.856	4.53	4.46	4.45	5.09/4.97
Yb	1.975	1.950	1.877	1.840	3.48	3.45	3.31	4.04/3.88

Experimental values [76]: R_e(Å): YbO 1.807; D_0(eV): EuO 4.80, YbO 4.29. AE DKH CCSD(T) values: R_e(Å): YbO 1.846; D_e(eV): YbO 3.27/3.12 [this work]

Table 2 Bond lengths R_e (in Å) and binding energies D_e (in eV) of selected lanthanide monohydrides LnH from PP(+CPP) CCSD(T) and PBE0 calculations in comparison with all-electron (AE) DKH2 PBE0 results without/with counter-poise correction of the basis set superposition error

Ln	R_e				D_e			
	CCSD(T)		PBE0		CCSD(T)		PBE0	
	PP	PP + CPP	PP + CPP	DKH	PP	PP + CPP	PP + CPP	DKH
Sm	2.159	2.155	2.133	2.106	1.82	1.78	1.73	2.04/2.03
Eu	2.154	2.148	2.124	2.105	1.76	1.72	1.65	2.02/2.00
Tm	2.118	2.097	2.069	2.046	1.49	1.38	1.23	1.55/1.50
Yb	2.116	2.091	2.061	2.049	1.44	1.32	1.16	1.58/1.53

Experimental values [76]: R_e(Å): YbH 2.053; D_0(eV)YbH $\leq$ 1.93 or $\leq$ 1.55. AE DKH CCSD(T) values: R_e(Å): YbH 2.055; D_e(eV): YbH 1.49/1.41 [this work]; R_e(Å): YbH 2.06; D_e(eV): YbH 1.38/1.35 [51]

experimental value by 0.03 and 0.07 Å, respectively, whereas for EuO no experimental value exists. The experimental EuO dissociation energy is bracketed by the smaller PP + CPP PBE0 and the larger DKH PBE0 binding energies, whereas both calculated binding energies are smaller than the experimental YbO dissociation energy. The DKH CCSD(T) bond length of YbO is 0.10 Å shorter than the corresponding PP + CPP result, whereas the PP + CPP CCSD(T) binding energy is 0.33 eV higher than the counter-poise corrected DKH CCSD(T) result. We note that the PP + CPP CCSD(T) bond length of EuO agrees within 0.001 Å with the value obtained from SPP CISD + Q calculations [42] and within 0.04 Å with a SPP MRCI + Q result using larger basis sets [43]. Most likely the disagreements for YbO are partly due to the configurational mixing present in the ground state, which might also be reflected by a DKH PBE0 Mulliken-f-population on Yb of 13.78, deviating from the ideal value of 14. We note that also for EuO a DKH PBE0 Mulliken-f-population smaller than the ideal value of 7, i.e., 6.84, is obtained. These lower f-populations are in line with results from recent B3LYP SPP calculations with an explicit treatment of the 4f-shell, where values of 6.86 and 13.83 were obtained for EuO and YbO, respectively [52]. They lead to a decrease in the Eu and Yb radii and thus to smaller bond distances. Despite the appealing ionic model for the electronic structure, YbO does not seem to be a valid test system for the f-in-core PP approach.

3.3.2 *Lanthanide monohydrides*

The lanthanide monohydrides of Sm, Eu, Tm and Yb are best described by a $[4f^n]\sigma^2\sigma^1$ superconfiguration (n = 6, 7, 13, 14 for Sm, Eu, Tm, Yb, respectively) and a $^2\Sigma^+$ valence substate. The 4f-in-core PP approach treats these molecules as 11 valence electron systems. The results for bond lengths and binding energies are listed in Table 2. The PP + CPP PBE0 bond lengths are 0.01–0.03 Å longer than the DKH PBE0 values. For YbH the calculated results bracket the experimental value. The PP + CPP PBE0 binding energies underestimate the DKH PBE0 values significantly, i.e. by 0.3–0.4 eV. All theoretical values are below the experimental upper bound for the dissociation energy. At the CCSD(T) level, the calculated PP + CPP YbH binding energy is only 0.09 eV below the counter-poise corrected DKH value; however, the PP + CPP YbH bond length is 0.036 Å longer than the DKH value. The DKH PBE0 (HF) Mulliken-f-population on Yb is 13.97 (13.99) in good agreement with the value of 14 modeled by the f-in-core PP for divalent Yb with a filled 4f-shell.

3.3.3 *Lanthanide monofluorides*

A $[4f^n]\sigma^2\sigma^2\pi^4\sigma^1$ superconfiguration and a $^2\Sigma^+$ valence substate was considered for the lanthanide monofluorides of Sm, Eu, Tm, and Yb (n = 6, 7, 13, 14 for Sm, Eu, Tm,

Table 3 Bond lengths R_e (in Å) and binding energies D_e (in eV) of selected lanthanide monofluorides LnF from PP(+CPP) CCSD(T) and PBE0 calculations in comparison with all-electron (AE) DKH2 PBE0 results without/with counter-poise correction of the basis set superposition error

Ln	R_e				D_e			
	CCSD(T)		PBE0		CCSD(T)		PBE0	
	PP	PP + CPP	PP + CPP	DKH	PP	PP + CPP	PP + CPP	DKH
Sm	2.102	2.091	2.079	2.065	5.65	5.64	5.58	5.93/5.82
Eu	2.096	2.083	2.068	2.068	5.58	5.57	5.49	5.84/5.73
Tm	2.057	2.029	2.003	1.993	5.20	5.15	4.91	5.36/5.22
Yb	2.052	2.031	2.001	2.009	5.10	5.03	4.76	5.26/5.11

Experimental values [76, 77, 78]: R_e(Å): YbF 2.016; D_0(eV): SmF 5.46, 5.81; EuF 5.42, 5.60; TmF 5.25; YbF 4.80, 5.00. AE DKH CCSD(T) values: R_e(Å): YbF 2.032; D_e(eV): YbF 5.13/5.03 [this work]; R_e(Å): EuF 2.08, YbF 2.03; D_e(eV): EuF 5.44/(5.34), YbF 4.82/(4.72) [51]

Table 4 Bond lengths $r_{Ln–H}$ (in Å) and bond angles $\varphi_{H–Ln–H}$ (in °) of LnH_2 from PP(+CPP) CCSD(T) and PBE0 calculations in comparison with all-electron (AE) DKH2 PBE0 results

Ln	$R_{Ln–F}$				$\varphi_{H–Ln–H}$			
	CCSD(T)		PBE0		CCSD(T)		PBE0	
	PP	PP + CPP	PP + CPP	DKH	PP	PP + CPP	PP + CPP	DKH
Sm	2.185	2.177	2.151	2.133	120.6	119.9	113.6	114.7
Eu	2.177	2.167	2.137	2.124	122.0	121.0	114.3	114.0
Tm	2.131	2.097	2.060	2.059	132.3	126.6	117.5	122.0
Yb	2.127	2.086	2.043	2.044	134.5	127.2	117.7	119.4

AE DKH CCSD(T) values: $R_{Ln–H}$(Å): YbH_2 2.065; $\varphi_{H–Ln–H}$(°): YbH_2 127.2 [this work]

Yb, respectively). The results for bond lengths and binding energies are listed in Table 3. The agreement between PP + CPP PBE0 and DKH PBE0 results for these tighter and more ionic bonds is better than for the weaker bonded and less ionix monohydrides. PP + CPP PBE0 and DKH PBE0 bond lengths agree within 0.01 Å, whereas the PP + CPP PBE0 binding energies are about 0.25–0.35 eV (4–7%) lower than the DKH PBE0 values. Both theoretical results underestimate the experimental YbF bond length by about 0.01–0.02 Å. The agreement between experimental dissociation energies and calculated binding energies is typically better than 0.3 eV. Experimental values often differ by a similar amount. At the CCSD(T) level, the PP + CPP and counter-poise corrected DKH binding energies of YbF agree within 0.01 eV, and the PP + CPP and DKH bond lengths within 0.001 Å. The DKH PBE0 (HF) Mulliken-f-population on Yb is 13.95 (14.00) indicating that the application of the f-in-core PP for divalent Yb is valid. A quite good agreement is also obtained with the AE DKH CCSD(T) results of Heiberg et al. [51], e.g. for EuO the PP + CPP and DKH bond lengths agree within 0.01 Å and the binding energies within 0.1 eV.

3.3.4 Lanthanide dihydrides and difluorides

Our structural results for the lanthanide dihydrides LnH_2 and difluorides LnF_2 are summarized in Tables 4 and 5, respectively. The Ln–H and Ln–F PP + CPP PBE0 and DKH PBE0 bond lengths agree within 0.02 and 0.01 Å for dihydrides and difluorides, respectively. The bond angles agree within 5°, which is still quite satisfactory in view of the flat bending energy profile and the possible steric influence of the non-spherical 4f-shell in the DKH PBE0 calculations. We note, however, that due to artefacts, e.g. the non-degeneracy of degenerate determinants at the DFT level [50], as well as the underlying single determinant description the DKH PBE0 results are not necessarily more reliable than the PP + CPP PBE0 results. At the CCSD(T) level of theory, the PP + CPP Yb–H bond length is only 0.02 Å longer than the DKH value, and the bond angles turn out to agree.

The bond energies of the lanthanide dihydrides LnH_2 and difluorides LnF_2 are listed in Table 6. The PP + CPP PBE0 values are lower than the DKH PBE0 results by only about 0.3 and 0.2 eV, respectively. The CCSD(T) bond energy of YbH_2 obtained from the PP + CPP calculations

Table 5 Bond lengths r_{Ln-F} (in Å) and bond angles φ_{F-Ln-F} (in °) of LnF_2 from PP(+CPP) CCSD(T) and PBE0 calculations in comparison with all-electron (AE) DKH2 PBE0 results

Ln	R_{Ln-F}				φ_{F-Ln-F}			
	CCSD(T)		PBE0		CCSD(T)		PBE0	
	PP	PP + CPP	PP+ CPP	DKH	PP	PP + CPP	PP + CPP	DKH
Sm	2.150	2.139	2.117	2.112	124.8	123.8	119.1	121.9
Eu	2.143	2.128	2.105	2.102	125.9	124.7	120.6	115.0
Tm	2.094	2.062	2.029	2.021	133.0	128.0	122.3	116.9
Yb	2.096	2.058	2.025	2.027	134.8	128.5	122.2	117.6

Experimental values [79]: EuF_2 $R(Eu-F) = 2.20 \pm 0.05$ Å AE DKH CASSCF/MRCI values: R_{Ln-F}(Å): YbF_2 2.048; φ_{F-Ln-F}(°): YbF_2 124.1; (note that a $^3A_1$ state with $4f^{13}$ configuration on Yb is found to be 0.33 eV lower in energy: R_{Ln-F}(Å): YbF_2 1.947; φ_{F-Ln-F}(°): YbF_2 119.4) [this work]

Table 6 Bond energies (eV) of Ln–H and Ln–F bonds of LnH_2 and LnF_2, respectively, from PP(+CPP) CCSD(T) and PBE0 calculations in comparison with all-electron (AE) DKH2 PBE0 results without/with counter-poise correction of the basis set superposition error

Ln	LnH_2				LnF_2			
	CCSD(T)		PBE0		CCSD(T)		PBE0	
	PP	PP + CPP	PP + CPP	DKH	PP	PP	PP + CPP	DKH
Sm	2.15	2.12	2.02	2.13/2.12	5.79	5.79	5.69	5.89/5.79
Eu	2.11	2.08	1.98	2.17/2.15	5.74	5.74	5.63	5.80/5.78
Tm	1.95	1.87	1.70	1.98/1.94	5.47	5.44	5.28	5.55/5.51
Yb	1.91	1.83	1.66	1.99/1.94	5.40	5.36	5.18	5.49/5.35

AE DKH CCSD(T) values: YbH_2 1.98/1.90 [this work]

is only 0.07 eV lower than the counter-poise corrected DKH reference value.

It is obvious from the molecular studies that the agreement between PP + CPP and DKH calculations is somewhat better at the CCSD(T) level than at the PBE0 level. One reason deserving further exploration might be that the radial overlap of electronic shells treated as core and valence is quite big for LPPs and nonlinear core-corrections would be needed [55]. No attempts to include such terms for energy-consistent PPs have been made so far to our knowledge.

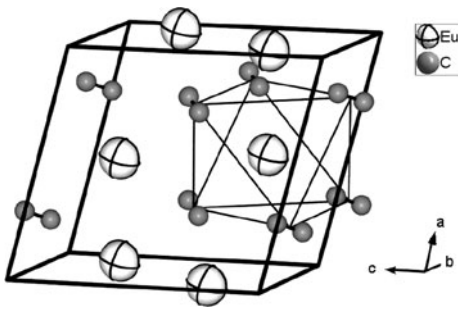

Fig. 5 EuC_2 in the monoclinic ThC_2 type structure. The Eu ions are sixfold coordinated (distorted octahedral) by carbon dumbbells and vice versa

3.4 Crystalline lanthanide dicarbides

An additional advantage of the new basis sets over the (7s6p5d)/[5s4p3d] basis sets originally published with the PPs [12] is that subsets, i.e. the primitive (4s4p3d) or (5s5p4d) sets as well as contracted sets derived from these, can be used in solid state calculations, e.g. using codes such as CRYSTAL [27]. As a first application we studied the lanthanide dicarbides (LnC_2) and focussed especially on the question of the valency of the lanthanide atoms in these systems. The calculations were carried out with the CRYSTAL06 program package [27] at the DFT level, and several density functionals supported by the program were applied. For the lanthanide atoms, 4f-in-core PPs with (5s5p4d)/[3s3p3d] valence basis sets of triple-zeta quality were used (divalent: [this work], trivalent [19]). Since large carbon basis sets cause linear dependencies for the dicarbide systems, we used Pople's standard 6-21G basis sets [56] as provided in the CRYSTAL06 basis set library. All free cell parameters as well as relative positions of the atoms inside the unit cells were fully optimized.

So far all solid lanthanide dicarbides, except PmC_2, have been synthesized and their cell parameters were determined. Except for EuC_2, which crystallizes in the

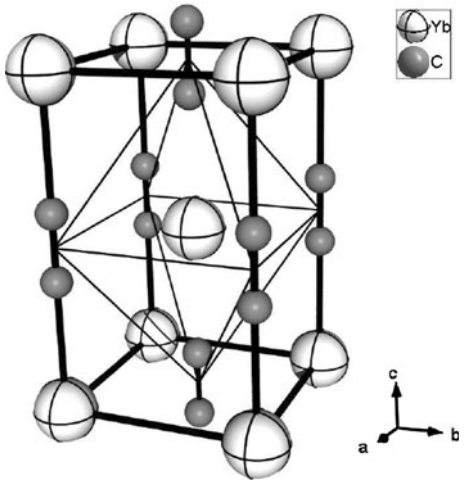

Fig. 6 YbC_2 in the tetragonal CaC_2 type structure. The Yb ions are sixfold coordinated (octahedral) by carbon dumbbells and vice versa

ThC_2 type structure (C2/c, $Z = 4$, monoclinic, cf. Fig. 5), all other lanthanide dicarbides possess CaC_2 type structure (I4/mmm, $Z = 2$, tetragonal, cf. Fig. 6). Here Z denotes the number of LnC_2 units in the crystallographic unit cell. Additional information on the space groups and symmetry of crystals can be found in the "*International Tables for Crystallography*" [57]. The structural data for the monoclinic modification of EuC_2 was first reported in 2006 by Wandner et al. [58]. Furthermore, several physical properties of the EuC_2 system, e.g. magnetic susceptibility or electrical conductivity, have recently been published [59].

In Fig. 7, the volumes per LnC_2 unit V/Z in the unit cell of the crystal are plotted against the atomic number of the rare-earth atoms. The experimentally determined volumes of the lanthanide dicarbides decrease almost linearly over

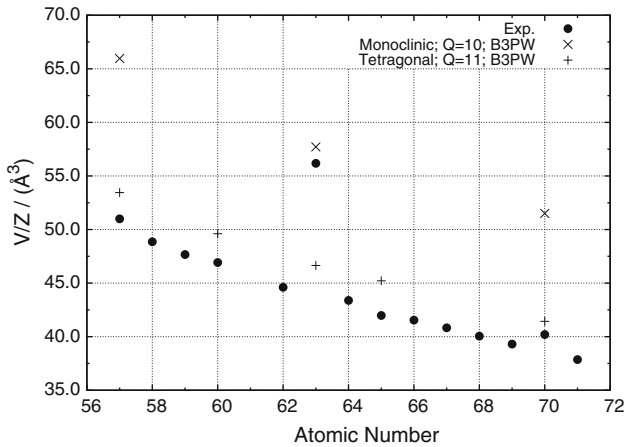

Fig. 7 Volumes of the unit cells per formula unit V/Z of several lanthanide dicarbides in tetragonal and monoclinic modifications from DFT (B3PW) calculations for periodic systems in comparison with experimental data. Calculations were done with CRYSTAL06 [27]

the lanthanide series; however, the corresponding volume of one EuC_2 unit does not fit into this trend. The same also holds for YbC_2, but the deviation is not that large here. The lanthanide dicarbides except EuC_2 and YbC_2 consist of Ln^{3+} cations as well as C_2^{2-} anions and one electron in the conduction band ($Ln^{3+}C_2^{2-}(e^-)$). On the basis of magnetic susceptibility measurements and ^{151}Eu Mössbauer spectroscopy, it was concluded that EuC_2 contains divalent Eu^{2+} cations and the C_2^{2-} dumbbells as anionic counterparts ($Eu^{2+}C_2^{2-}$) [59].

The results of the calculations of the tetragonal lanthanide dicarbides using 4f-in-core PPs for trivalent lanthanide ions will be discussed first. Tetragonal LaC_2 is considered as a benchmark system, since this compound actually contains trivalent La [60]. We also calculated the optimized structures of tetragonal NdC_2 and TbC_2 in order to confirm that our approach is appropriate along the lanthanide series. The B3PW functional [61–65] yielded the best results within our approximations and is discussed below. The corresponding results are summarized in Tables 7 and 8, and the calculated volumes of the unit cell per formula unit are plotted in Fig. 7 together with the experimental values. The calculations with other density functionals such as B3LYP [61, 66], BP86 [67, 68], PBE [30], and PWGGA [69] are summarized in the supplementary material. These functionals lead to similar results and the same trends.

The optimized lattice parameters for the tetragonal case using trivalent Ln 4f-in-core PPs are in good agreement with the experimental values, i.e. the relative errors are

Table 7 Calculated lattice parameters a and c (Å), volumes of the unit cell per formula unit V/Z (Å^3), and the C–C distance d_{C-C} (Å) of the tetragonal modifications of LaC_2, NdC_2, EuC_2, TbC_2, and YbC_2 from DFT calculations using the B3PW functional as provided in the CRYSTAL06 program package

LnC_2	a	c	V/Z	d_{C-C}
LaC_2				
Exp. [60]	3.937	6.580	50.99	1.284
B3PW	4.018	6.623	53.46	1.299
NdC_2				
Exp. [73]	3.827	6.407	46.92	1.302
B3PW	3.912	6.483	49.61	1.304
EuC_2				
B3PW	3.831	6.356	46.64	1.308
TbC_2				
Exp. [74]	3.678	6.206	41.98	1.291
B3PW	3.788	6.300	45.20	1.309
YbC_2				
Exp. [75]	3.635	6.113	40.39	1.281
B3PW	3.677	6.128	41.43	1.311

Table 8 Calculated lattice parameters a, b, c (Å) and β (°), volumes of the unit cell per formula unit V/Z (Å^3) and the C–C distance d_{C-C} (Å) of the monoclinic modifications of LaC_2, EuC_2 and YbC_2 from DFT calculations using the B3PW functional as provided in the CRYSTAL06 program package

LnC_2	a	b	c	β	V/Z	d_{C-C}
LaC_2						
B3PW	7.362	4.839	7.837	109.07	65.97	1.272
EuC_2						
Exp. [70]	7.011	4.411	7.595	106.92	56.18	1.199
B3PW	7.073	4.390	7.768	106.84	57.71	1.271
YbC_2						
B3PW	6.785	4.225	7.514	106.99	51.50	1.270

typically less than 3.0%. The distances of the carbon atoms in the C_2 units are also reproduced very well. The maximum absolute error is 0.030 Å (2.3%) for YbC_2. The volumes of the unit cells per formula unit decrease over the lanthanide row from LaC_2 to LuC_2. The calculated reduction in the volume is similar to the experimentally observed one and shows an almost linear behaviour (cf. Fig. 7). This set of calculations also contained the optimization of a hypothetical modification of tetragonal EuC_2 that contains trivalent Eu ions. This EuC_2 modification would fit well into the trend obtained for the other lanthanide dicarbides.

The calculation of the monoclinic EuC_2 crystal using the divalent Eu 4f-in-core PP also leads to satisfactory results. Usually, doubly charged lanthanide ions have larger atomic radii than the corresponding triply charged ions and thus the doubly charged Eu ions require more space within the unit cell of the crystal. Therefore, the carbon dumbbells turn away from the z-axis and the EuC_2 crystal becomes monoclinic. The experimental C–C bond length in EuC_2 equals 1.199 Å [70], i.e., nearly the same value as for the length of the "standard" C–C triple bond in acetylene (1.205 Å) [71, 72]. Hence, this monoclinic modification of EuC_2 can be described as $Eu^{2+}C_2^{2-}$. The calculated lattice constants deviate from the experimental values for a, b, c, and β by 0.062 Å (0.9%), 0.021 Å (0.5%) 0.073 Å (0.9%), and 1.13° (1.9%), respectively.

We also calculated hypothetical monoclinic structures of LaC_2 and YbC_2 using the corresponding 4f-in-core PPs for divalent La and Yb. The calculated monoclinic unit cell volumes are substantially ($\approx$24%) larger than those of the tetragonal crystals, whereas our calculated unit cell volumes of the tetragonal crystal structures are only slightly larger ($\approx$3–8%) than the experimental values. Similar to the tetragonal case, the unit cell volumes of the monoclinic crystals exhibit a decrease along the lanthanide series.

Within the approximations we have made, the results are consistent and also match the hypotheses of the experimentalists. From the theoretician's point of view, the monoclinic EuC_2 crystal contains Eu ions with a valency close to two, whereas tetragonal YbC_2 crystal contains Yb ions with a valency close to three. The fact that the experimental unit cell volume of tetragonal YbC_2 is slightly larger than expected from the trend for lanthanide dicarbides with trivalent metal ions might indicate a weak admixture of a $4f^{14}$ subconfiguration (divalent case) to the leading $4f^{13}$ subconfiguration (trivalent case). Similar to the situation for molecular YbO, such details of the electronic structure cannot be dealt with quantitatively with lanthanide 4f-in-core PPs. Nevertheless, the calculations demonstrate that besides their use in molecular quantum chemical studies the 4f-in-core PPs can also be useful tools for investigations into crystalline systems, avoiding many computational problems related to the partially occupied 4f shell.

4 Conclusion

New valence basis sets with various primitive sizes and contraction patterns for approximately valence double- to quadruple-zeta quality for scalar-relativistic 4f-in-core pseudopotentials modeling divalent lanthanide atoms were generated. Compact (4s4p3d) and (5s5p4d) primitive basis sets are suitable for calculations of crystalline solids with Ln^{2+} ions and (6s5p4d) and (7s6p5d) extended sets containing diffuse functions are intended for atomic and molecular calculations on neutral or low-charged systems. Compared to the original (7s6p5d) primitive sets, the new (7s6p5d) extended sets exhibits an order of magnitude smaller errors with respect to the Hartree-Fock limit for the atomic (mostly ground state) $5s^25p^66s^2$ valence subconfiguration, e.g. for the $Yb\,^1S$ ground state the deviations from the Hartree-Fock limit are 1.68 and 0.14 eV, respectively. The additional errors due to contraction of the basis sets stay below 0.01 eV. The results of test calculations of atomic ionization potentials and geometry optimizations of several lanthanide compounds using 4f-in-core pseudopotentials with the new valence basis sets show good agreement with available experimental data as well as with all-electron data derived from calculations using the Doulgas-Kroll-Hess scalar-relativistic Hamiltonian. Especially the calculations of the first and second ionization potentials of the lanthanides lead to very good results when core-polarization potentials are included, i.e. mean absolute errors are 0.09 eV (1.5%) for the first and 0.13 eV (1.2%) for the second ionization potentials. The mean absolute errors at the PP + CPP PBE0 level with respect to DKH PBE0 reference data for 18 bond lengths, 8 bond angles and 18 binding/bond energies of the test molecules are 0.014 Å, 4.0° and 0.28 eV,

respectively. An additional advantage of the improved basis sets besides their lower total valence energies is their applicability to crystalline solids. This is illustrated by calculations on the dicarbides of Eu and Yb, assigning a valency of II to Eu in EuC_2 and of III to Yb in YbC_2 in agreement with experimental evidence. Overall, the application of 4f-in-core pseudopotentials in calculations of divalent lanthanide molecular or crystalline systems is a profitable choice regarding CPU time. The loss of accuracy is for most purposes tolerable, as long as the 4f orbitals do not participate too much in chemical bonding or a configurational mixing takes place. Finally, the present work completes the development of lanthanide and actinide f-in-core pseudopotentials and corresponding molecular and crystal orbital basis sets.

References

1. Pyykkö P (1988) Chem Rev 88:563
2. Dolg M, Stoll H (1996) Electronic structure calculations for molecules containing lanthanide atoms. In: Gschneidner KA, Eyring L (eds) Handbook on the physics and chemistry of rare earths, vol 22. Elsevier Science B.V., Amsterdam
3. Dolg M, Cao X (2003) The relativistic energy-consistent ab initio pseudopotential approach. In: Hirao K, Ishikawa Y (eds) Recent advances in relativistic molecular theory. World Scientific, New Jersey
4. Hay PJ, Wadt WR (1985) J Chem Phys 82:270
5. Wadt WR, Hay PJ (1985) J Chem Phys 82:284
6. Hay PJ, Wadt WR (1985) J Chem Phys 82:299
7. Pyykkö P, Stoll H (1999) In: Hincliffe A (ed) R S C Spec Period Rep, chemical modelling, applications and theory, vol 1, Cambridge, pp 239–305
8. Cao X, Dolg M (2010) In: Barysz M, Ishikawa Y (eds) Relativistic methods for chemists. Challenges and advances in computational physics, vol. 10 Springer, Heidelberg, pp 215–278
9. Dolg M, Stoll H, Preuss H (1989) J Chem Phys 90:1730
10. Cao X, Dolg M (2001) J Chem Phys 115:7348
11. Froese-Fischer C (1977) The Hartree–Fock method for atoms. Wiley, New York; program MCHF77, modified for pseudopotentials and quasirelativistic calculations by Dolg M (1988,1995)
12. Dolg M, Stoll H, Savin A, Preuss H (1989) Theor Chim Acta 75:173
13. Dolg M, Stoll H, Preuss H (1993) Theor Chim Acta 85:441
14. Hülsen M, Weigand A, Dolg M (2009) Theor Chem Acc 122:23
15. Moritz A, Cao X, Dolg M (2007) Theor Chem Acc 117:473
16. Moritz A, Cao X, Dolg M (2007) Theor Chem Acc 118:845
17. Moritz A, Dolg M (2008) Theor Chem Acc 121:297
18. Pyykkö P (1987) Inorg Chim Acta 139:243
19. Yang J, Dolg M (2005) Theor Chem Acc 113:212
20. Weigand A, Cao X, Yang J, Dolg M (2010) Theor Chem Acc 126:117
21. Pitzer RM, Atomic electronic structure code ATMSCF. The Ohio State University, Columbus
22. Werner HJ, Knowles PJ, Lindh R, Manby FR, Schütz M et al (2006) MOLPRO, version 2006.1, a package of ab initio programs, Cardiff, UK
23. http://www.theochem.uni-stuttgart.de/pseudopotentials
24. Wang Y, Dolg M (1998) Theor Chem Acc 100:124
25. Müller W, Flesch J, Meyer W (1984) J Chem Phys 80:3297
26. Müller W, Meyer W (1984) J Chem Phys 80:3311
27. Dovesi R, Saunders VR, Roetti R, Orlando R, Zicovich-Wilson CM, Pascale F, Civalleri B, Doll K, Harrison NM, Bush IJ, D'Arco P, Llunell M (2006) CRYSTAL06 user's manual, University of Torino, Torino
28. Martin WC, Zalubas R, Hagan L (1978) Atomic energy levels—the rare earth elements, NSRDS-NBS 60, Washington, DC
29. Adamo C, Barone V (1999) J Chem Phys 110:6158
30. Perdew JP, Burke K, Ernzerhof M (1996) Phys Rev Lett 77:3865
31. Dunning TH Jr (1989) J Chem Phys 90:1007
32. Kendall RA, Dunning TH Jr, Harrison RJ (1992) J Chem Phys 96:6796
33. Douglas M, Kroll NM (1974) Ann Phys 82:89
34. Hess BA (1986) Phys Rev A 33:3742
35. Dolg M (2009) AIP conference proceedings, ICCMSE 2009, in press
36. de Jong WA, Harrison RJ, Dixon DA (2001) J Chem Phys 114:48
37. Boys SF, Bernardi F (1970) Mol Phys 19:553
38. Link P, Ruschewitz U, Hülsen M, Dolg M (2010) in preparation
39. Field RW (1982) Ber Bunsenges Phys Chem 86:771
40. Dolg M, Stoll H (1989) Theor Chim Acta 75:369
41. Dolg M, Stoll H, Preuß H (1991) J Mol Struct (THEOCHEM) 235:67
42. Dolg M, Stoll H, Preuß H (1990) Chem Phys 148:219
43. Cao X, Liu WJ, Dolg M (2002) Sci China Ser B 45:91
44. Dolg M, Stoll H, Preuß H (1992) Chem Phys 165:21
45. Dolg M, Stoll H, Flad HJ, Preuss H (1992) J Chem Phys 97:1162
46. Cao X, Liu W, Dolg M (2001) Sci China B 31:481; engl. 45:91
47. Wang SG, Schwarz WHE (1995) J Phys Chem 99:11687
48. Wang SG, Pan DK, Schwarz WHE (1995) J Chem Phys 102:9296
49. Liu W, Hong G, Dai D, Li L, Dolg M (1997) Theor Chem Acc 96:75
50. Liu W, Dolg M, Li L (1998) J Chem Phys 108:2886
51. Heiberg H, Gropen O, Laerdahl JK, Swang O, Wahlgren U (2003) Theor Chem Acc 110:118
52. Wu ZJ, Guan W, Meng J, Su ZM (2007) J Clust Sci 18:444
53. Infante I, Gagliardi L, Wang XF, Andrews L (2009) J Phys Chem A 113:2446
54. McDonald SA, Rice RF, Field RW, Linton C (1990) J Chem Phys 93:7676
55. Louie SG, Froyen S, Cohen ML (1982) Phys Rev B 26:1738
56. Binkley JS, Pople JA, Hehre WJ (1980) J Am Chem Soc 102:939
57. Hahn T (2002) In: Hahn T (ed) International tables for crystallography, vol A, 5th edn. Kluwer Acad Publ, Dordrecht
58. Wandner D, Ruschewitz U, Abd-Elmeguid M, Ahmida MA, Heyer O (2006) Z Anorg Allg Chem 632:2099
59. Wandner D, Link P, Heyer O, Mydosh J, Ahmida MA, Abd-Elmeguid MM, Speldrich M, Lueken H, Ruschewitz U (2010) Inorg Chem 49:312
60. Jones DW, McColm IJ, Yerkess J (1991) J Solid State Chem 92:301
61. Becke AD (1993) J Chem Phys 98:5648
62. Perdew JP (1991) Electronic structure of solids. Akademie, Berlin
63. Perdew JP, Yue W (1986) Phys Rev B 33:8800
64. Perdew JP, Wang Y (1989) Phys Rev B 40:3399
65. Perdew JP, Wang Y (1992) Phys Rev B 45:13244
66. Lee C, Yang W, Parr RG (1988) Phys Rev B 37:785
67. Becke AD (1988) Phys Rev A 38:3098
68. Perdew JP (1986) Phys Rev B 33:8822
69. Perdew JP, Chevary JA, Vosko SH, Jackson KA, Pederson MR, Singh DJ, Fiolhais C (1992) Phys Rev B 46:6671
70. Ruschewitz U (2010) Private communication
71. Overend J (1960) Trans Faraday Soc 56:310
72. Pyykkö P, Riedel S, Patzschke M (2005) Chem Eur J 11:3511

73. Jones DW, McColm IJ, Steadman R, Yerkess J (1986) J Solid State Chem 62:172
74. Atoji M (1967) J Chem Phys 46:1891
75. Link P (2010) Private communication
76. Huber KP, Herzberg G (1979) Molecular spectra and molecular structure. IV. Constants of diatomic molecules. Van Nostrand, New York
77. Kleinschmidt PD, Lau KH, Hildenbrandt DL (1981) J Chem Phys 74:653
78. Lee HU, Zare RN (1977) J Molec Spectr 64:233
79. Hastie JW, Hauge RH, Margrave JL (1971) High Temp Sci 3:56